(12)

DTNSRDC-83/055

DAVID W. TAYLOR NAVAL SHIP RESEARCH AND DEVELOPMENT CENTER

Bethesda, Maryland 20084

OPTIMUM FOREBODY SHAPING FOR AXISYMMETRIC SUBMERSIBLES WITH TURBULENT BOUNDARY LAYERS AND BLC AFTERBODIES

by

Benjamin J. Neumann

APPROVED FOR PUBLIC RELEASE: DISTRIBUTION UNLIMITED

AVIATION AND SURFACE EFFECTS DEPARTMENT
RESEARCH AND DEVELOPMENT REPORT

July 1983

DTNSRDC-83/055

MAJOR DTNSRDC ORGANIZATIONAL COMPONENTS

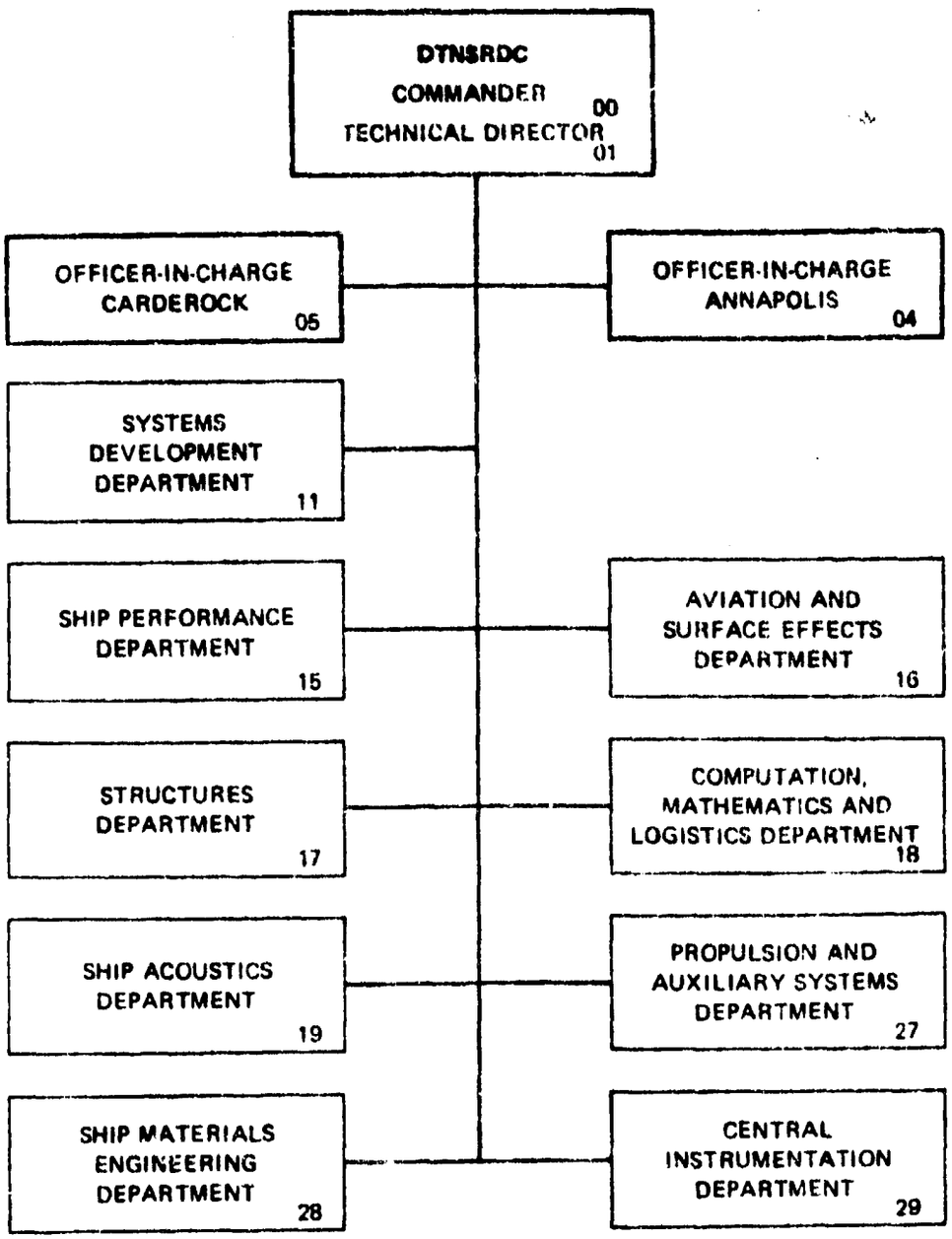

UNCLASSIFIED

SECURITY CLASSIFICATION OF THIS PAGE (When Data Entered)

REPORT DOCUMENTATION PAGE	READ INSTRUCTIONS BEFORE COMPLETING FORM
1. REPORT NUMBER: DTNSRDC-83/055	2. GOVT ACCESSION NO.: AD-A130 950
	3. RECIPIENT'S CATALOG NUMBER:
4. TITLE (and Subtitle): OPTIMUM FOREBODY SHAPING FOR AXISYMMETRIC SUBMERSIBLES WITH TURBULENT BOUNDARY LAYERS AND BLC AFTERBODIES	5. TYPE OF REPORT & PERIOD COVERED: Final Report Oct 1982 - Jan 1983
	6. PERFORMING ORG. REPORT NUMBER: Aero Report 1284
7. AUTHOR(s): Benjamin J. Neumann	8. CONTRACT OR GRANT NUMBER(s):
9. PERFORMING ORGANIZATION NAME AND ADDRESS: David Taylor Naval Ship Research and Development Center Bethesda, MD 20084	10. PROGRAM ELEMENT, PROJECT, TASK AREA & WORK UNIT NUMBERS: Program Element 62702E Work Unit 1603-604
11. CONTROLLING OFFICE NAME AND ADDRESS: Defense Advanced Research Projects Agency 1400 Wilson Boulevard Arlington, VA 22209	12. REPORT DATE: July 1983
	13. NUMBER OF PAGES: 41
14. MONITORING AGENCY NAME & ADDRESS (if different from Controlling Office)	15. SECURITY CLASS. (of this report): UNCLASSIFIED
	15a. DECLASSIFICATION/DOWNGRADING SCHEDULE

16. DISTRIBUTION STATEMENT (of this Report)

APPROVED FOR PUBLIC RELEASE: DISTRIBUTION UNLIMITED

17. DISTRIBUTION STATEMENT (of the abstract entered in Block 20, if different from Report)

18. SUPPLEMENTARY NOTES

19. KEY WORDS (Continue on reverse side if necessary and identify by block number)

Boundary Layer
Boundary Layer Control
Axisymmetric Body
Transition Analysis Program System (TAPS)
Submersible

20. ABSTRACT (Continue on reverse side if necessary and identify by block number)

One objective of the Advanced Undersea Vehicle (AUV) program is to design a low drag vehicle. The approach ~~to this objective~~ in this investigation is boundary layer control by means of an annular suction slot located on the afterbody. Although wind tunnel data showed significant reduction in propulsive power over conventional shapes, an attempt was made to achieve further reduction by means of forebody shaping. Two methods were used to vary the

(Continued on reverse side)

DD FORM 1473 EDITION OF 1 NOV 65 IS OBSOLETE

UNCLASSIFIED

SECURITY CLASSIFICATION OF THIS PAGE (When Data Entered)

(Block 20 continued)

geometric parameters for this analysis. The direct method, based on the mathematical development of the Series 58 bodies, allows the definition of a shape by a fifth-order polynomial based on the four fundamental parameters of fineness ratio, nose radius of curvature, location of maximum thickness, and prismatic coefficient. The inverse method allows various velocity distributions to define the body shape. The shapes derived by this method have flat velocity distributions and show similar trends to the polynomial shapes (about 3-percent reduction in propulsive power). The range of fineness ratios analyzed was from 1 to 10 at a volume-based Reynolds number of 3.2 million. In the range of 2.5 to 8, fineness ratio did not affect propulsive power more than 6 percent. A maximum improvement of 3 percent was shown by varying the meridian section.

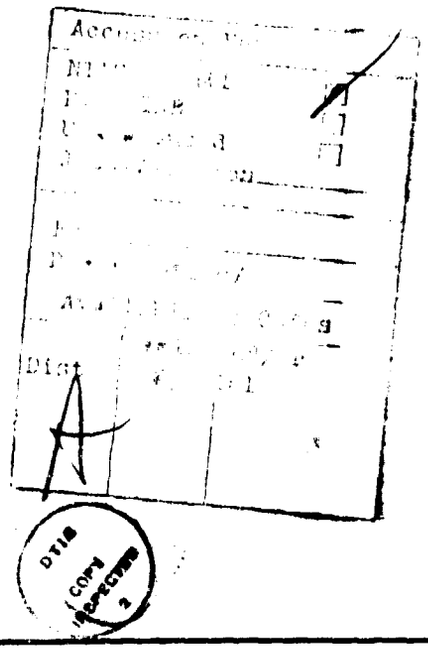

TABLE OF CONTENTS

LIST OF FIGURES

LIST OF TABLES

NOTATION

A	The surface area of a frustum, ft^2
C	Maximum radius of a body, ft, $C = d/2$
C_D	Drag coefficient
C_H	Head coefficient, H/q_o
C_Q	Mass flow coefficient
C_p	Pressure coefficient
Cp^*	Ideal forebody power coefficient
C_V	Prismatic coefficient, fraction of usable volume contain by the body, $C_V = \frac{4\nabla}{\pi d^2 \ell}$
d	Maximum diameter of body, ft
H	Fluid total head, lb/ft^2 gage
K_1	Maximum velocity ratio
K_2	Final velocity ratio
L, ℓ	Body length, ft
ℓ/d	Fineness ratio
M	Fraction of body length where body is thickest
n	Exponent used in velocity curve fit
P	Power, ft-lb/sec
p_s	Static pressure
q	Dynamic pressure, lb/ft^2, $q = 1/2\rho V^2$
R_o	Radius of curvature at the nose, ft
r_o	Nondimensional radius of curvature at the nose, $r_o = R_o \cdot \ell/d^2$
r_1	Body radius at the location of the boundary layer rake, ft
Re_∇	Reynolds number based on volume raised to the one third power, $Re_\nabla = \frac{V_o \nabla^{1/3}}{\nu}$
S	Surface distance, ft

V	Velocity, ft/sec
y	Height, ft
δ	Boundary layer height, ft
∇	Volume, ft^3, (for BLC bodies, the portion of the body volume upstream of the inlet location; otherwise total body volume)
θ	Angle between normal to body surface and the vertical, degrees
ρ	Density, $slugs/ft^3$
ν	Kinematic viscosity, ft^2/sec

Subscripts

i	Value at heights normal to body, y_i
1	Local conditions at station 1, the assumed inlet location
0	Free-stream conditions
te	Trailing edge of the body

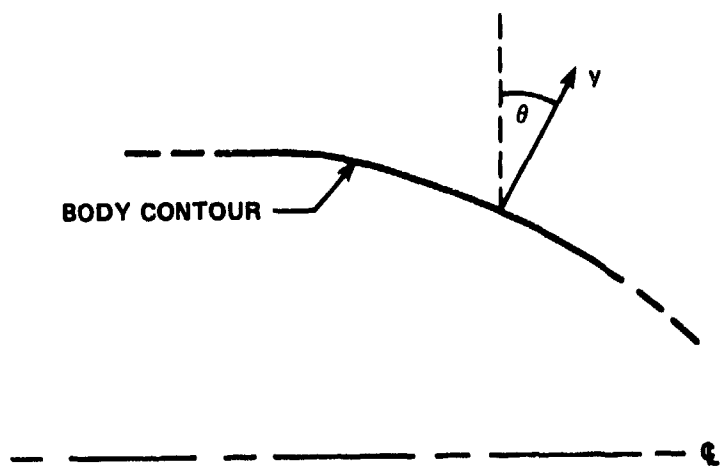

NOMENCLATURE

ABSTRACT

One objective of the Advanced Undersea Vehicle (AUV) program is to design a low drag vehicle. The approach to this objective in this investigation is boundary layer control by means of an annular suction slot located on the afterbody. Although wind tunnel data showed significant reduction in propulsive power over conventional shapes, an attempt was made to achieve further reduction by means of forebody shaping. Two methods were used to vary the geometric parameters for this analysis. The direct method, based on the mathematical development of the Series 58 bodies, allows the definition of a shape by a fifth-order polynomial based on the four fundamental parameters of fineness ratio, nose radius of curvature, location of maximum thickness, and prismatic coefficient. The inverse method allows various velocity distributors to define the body shape. The shapes derived by this method have flat velocity distributions and show similar trends as the polynomial shapes (about 3-percent reduction in propulsive power). The range of fineness ratios analyzed was from 1 to 10 at a volume-based Reynolds number of 3.2 million. In the range of 2.5 to 8, fineness ratio did not affect propulsive power more than 6 percent. A maximum improvement of 3 percent was shown by varying the meridian section.

ADMINISTRATIVE INFORMATION

This work was performed by the New Vehicle Office (Code 1603) of the Aviation and Surface Effects Department at the David W. Taylor Naval Ship Research and Development Center (DTNSRDC). The project was funded by the Defense Advanced Research Projects Agency (DARPA) under Program Element 62702E, DTNSRDC Work Unit 1603-604.

INTRODUCTION

One aspect of the Advanced Undersea Vehicle (AUV) program addresses the development of low-power requirements for an axisymmetric turbulent flow hydrodynamic body. The present concept uses the ingestion of the boundary layer fluid and the reenergization of the fluid to propel the vehicle. By ingesting the fluid at the proper location and with proper afterbody shaping, flow separation can be

avoided even with very full afterbodies. The ability to design full afterbodies without a power penalty has resulted in high prismatic coefficient bodies ($C_V > 0.8$) with low-power requirements. Analytical studies have been performed to develop body shapes for experimental verification in a wind tunnel.[1]* The body shape selected for this experiment uses a Reichardt nose and parallel mid-bodies which varied the body length-to-diameter ratio (4, 5, and 6); see Figure 1. The full afterbody shape was selected based on a preliminary design for the propulsor and shroud.

The three designs were experimentally evaluated in a wind tunnel[2] in an unpowered condition using a fan mounted downstream of the model connected by a duct to provide the suction air simulating the propulsor. Pressure measurements provided data to determine the power coefficients for the bodies at various suction flow rates. One of the many observations during the wind tunnel investigation was that the body with a fineness ratio 6 (i.e., length-to-maximum-diameter ratio) performed better than the lower fineness ratio bodies. This study was undertaken to verify the wind tunnel results and to determine if another shape could perform even better than the shapes selected for the wind tunnel experiments.

One way of assessing the performance of a vehicle is by calculating the power required to propel the vehicle at a constant speed, that is, propulsive power. An attempt was made to reduce propulsive power on the wind tunnel model by means of forebody shaping. It was believed that an efficient means of accelerating the fluid over the forebody such that boundary layer growth would be controlled would result in a reduction in required power. Forebody shaping to reduce drag had been investigated a number of times, but the feasibility of efficient afterbody boundary

---

*A complete listing of references is given on page 33.

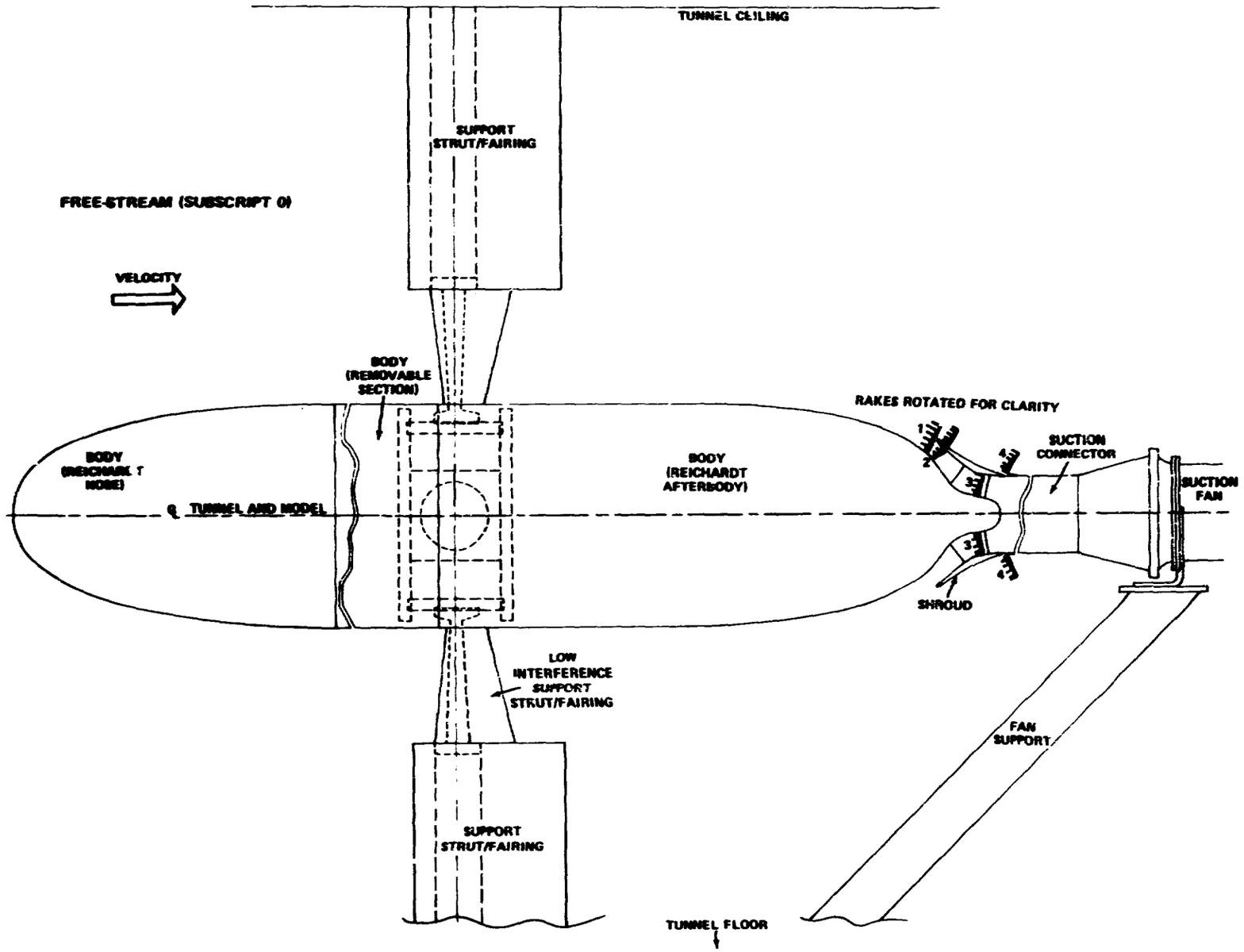

Figure 1 - Component Schematic of Boundary Layer Control Model Installed in Wind Tunnel

layer control, which was demonstrated earlier in the program, provides two new considerations that suggest a separate study. First, because separation is avoided, i.e., no form drag, the primary component of drag to be considered is skin friction. In addition, since an afterbody is required for boundary layer control, the analysis of the skin friction should be conducted only from the nose of the body to a point where an inlet would be placed. Second, only turbulent flow is of interest in this study whereas some other studies dealt with laminar flow. These two issues justified proceeding with a forebody shaping program at DTNSRDC. (See References 3 and 4 for details of other studies.)

EVALUATION CRITERIA

It is assumed that with a properly developed BLC aftbody the form drag will be negligible, external aftbody friction will be very small and its dependence on forebody geometry can be neglected, and the internal efficiency with which boundary layer fluid can be ingested, reenergized and exhausted is also independent of forebody geometry. These assumptions greatly simplify the problem of comparing the merits of different overall body geometries since they can be compared on the basis of boundary layer properties at an assumed propulsor inlet location and the details of aftbody internal and external shaping need not be considered.

The inlet location was selected as a point slightly upstream from the occurrence of boundary layer separation as determined from a calculation of the boundary layer development under the influence of the calculated potential-flow pressure distribution. By choosing to nondimensionalize results in terms of the body volume upstream of the chosen inlet location, it was found that the effect of small variations in the exact choice of inlet location was made negligible. (This choice

of reference volume was necessary in any case in order to avoid having to deal with the details of aftbody geometry.)

The quantity chosen as the measure of relative merit of the various body geometries is ideal forebody power coefficient, C_p^*, a nondimensional measure of the power required by an ideal propulsor to restore the boundary layer fluid at the chosen inlet location to free-stream total head.

This coefficient is defined as:

$$C_p^* = \frac{P^*}{q_o V_o \nabla^{2/3}} \tag{1}$$

where

$$P^* = \int_o^\delta V_i \, (q_o - H_i) \, dA_i \tag{2}$$

$$dA_i = 2\pi \, (r_i + y_i \cos \theta) \, dy \tag{3}$$

But

$$V_i \, dA_i = V_o \nabla^{2/3} \, dC_Q \tag{4}$$

Hence

$$C_p^* = \int_o^\delta (1 - C_{H_i}) \, dC_Q \tag{5}$$

The requisite boundary layer information, namely C_H as a function of C_Q, was obtained from the Transition Analysis Program System (TAPS)[5,6] which was also one of the primary tools used in the analysis and development of the earlier wind tunnel configurations. Correlation between TAPS and actual wind tunnel data has, to some degree, been completed. Very good comparisons between the

TAPS potential solution and pressure coefficient, $(p_{s_1} - p_{s_o})/q_o$, measurements have been found. In Figure 2, a sample plot shows the pressure distribution over the wind tunnel model ($\ell/d = 6$) with the TAPS prediction. Also, good agreement has been found between the predicted energy content of the fluid just upstream of the inlet and the measured energy (head profile). Predicted head profile is compared with the measured head profile in Figure 3. The head profile is presented by a head coefficient versus a mass flow coefficient; the latter is similar to the stream function concept, that is, the mass flow is constant between streamlines. This method of presentation is essential because the experimental data revealed significant variation of static pressure across the boundary layer. Since TAPS assumes uniform static pressure across the boundary layer, comparisons of H vs y and V vs y separately would suggest very poor correlation even though the actual correlation in terms of flow quantities needed for this study is excellent.

The wind tunnel model geometries were also analyzed by TAPS at the same conditions as the wind tunnel data points so that further correlation could be made between predictions and actual measurements. The wind tunnel models had a 13-tube rake of which 11 tubes were for total pressure and 2 were for static pressure measurements (Figure 4). This rake, located just forward of the inlet, is referred to as the boundary layer rake. The boundary layer rake measurements were integrated, as shown in Equations (1) through (5), in order to correlate the analysis with actual data. The results of this correlation showed very good agreement, as indicated in Table 1.

GEOMETRY DEVELOPMENT

In order to compare the different shapes and to understand their variation in performance, a method was sought which would allow the variation of geometric

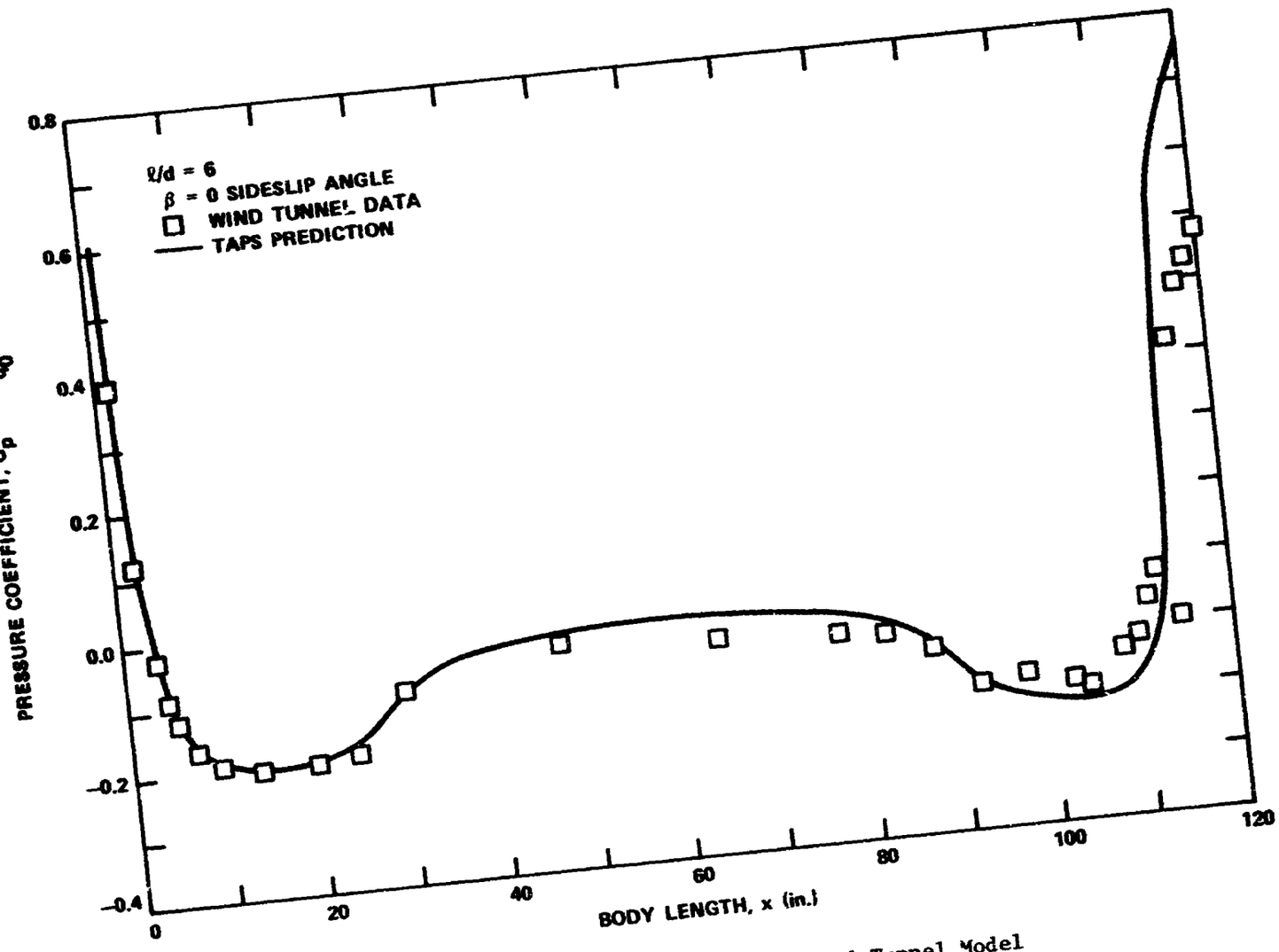

Figure 2 - Pressure Distribution Over Wind Tunnel Model

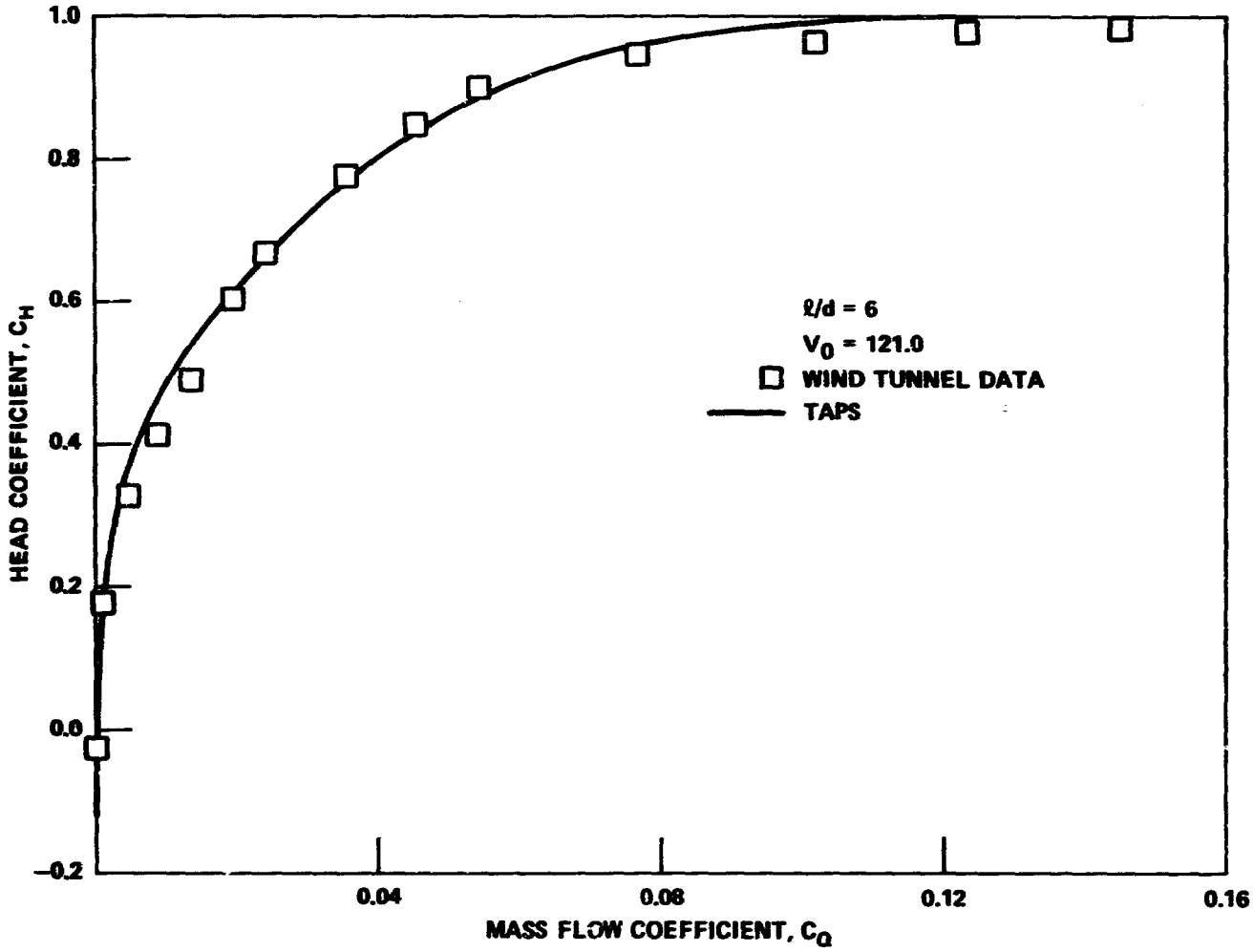

Figure 3 - Energy Content versus Mass Flow in Boundary Layer

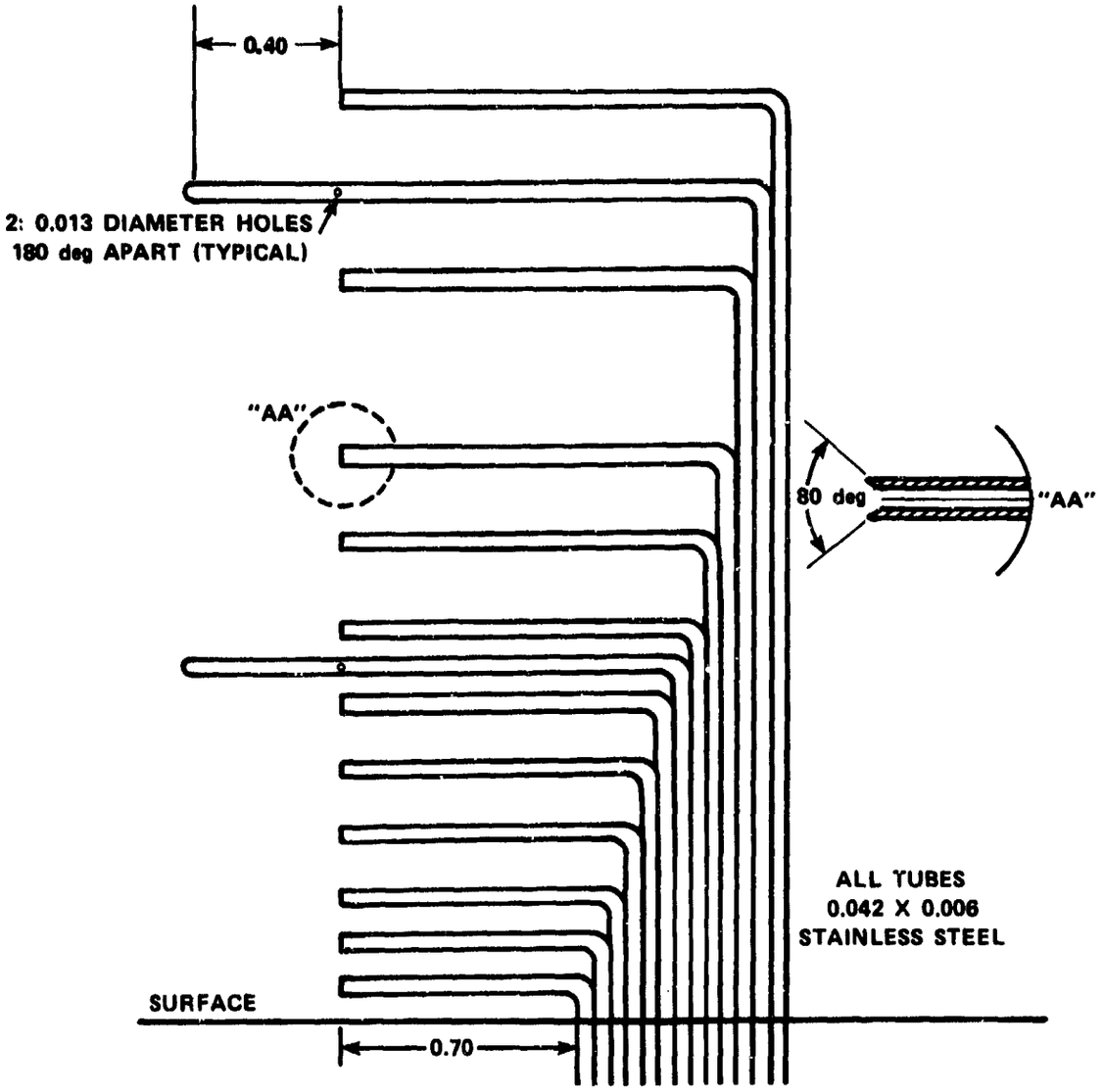

Figure 4 - Boundary Layer Rake Schematic

TABLE 1 - CORRELATION BETWEEN TAPS PREDICTION AND WIND TUNNEL DATA

Wind Tunnel Model, ℓ/d	Predicted C_p*	Measured C_p*	Variation (%)
6	0.0201	0.0206	2.5
5	0.0202	0.0200	1.1
4	0.0195	0.0193	1.0

parameters. These parameters include fineness ratio, prismatic coefficient, nose radius of curvature, and the location of maximum thickness. Two approaches are available to accomplish this. The first approach, the direct method, is to define a geometry based on the four parameters and then analyze its flow characteristic. The second approach, the inverse method, is to prescribe a velocity distribution and find the geometry that matches.

DIRECT METHOD

The direct method is a modification to the work done by Gertler and Landweber[7] in 1950. The problem simply stated: A polynomial is desired which defines the geometry of a body of revolution. It is desired that four parameters be available for the user to vary, thereby generating a family of geometrically similar bodies. The parameters are fineness ratio, prismatic coefficient, nose radius for curvature, and the location of maximum thickness. The equation takes the form:

$$y^2(x) = 2\, r_o\, R(x) + C^2 Q(x) + C_V P(x) \qquad (6)$$

where R(x), Q(x), and P(x) are fifth-order polynomials.

The one parameter that is not apparent, but of major importance, is the location of maximum thickness of the body, M. Due to the mathematical limitations of Equation (6), M was chosen to be 0.7 of the body length for all geometries

analyzed. The derivation of R(x), Q(x), and P(x) is shown in the appendix and is similar to the method presented in Reference 7.

The major portion of this study was done with geometries generated by the direct method. Certain restrictions are imposed in Equation (6) in order to ensure a smooth body. An example of these limitations is shown in Figures 5 and 6. Figure 5 shows a region within which only one point of zero slope exists on the body contour. This alone does not ensure a realistic geometry nor a smooth one. Figure 6 shows regions in which $y < 0$ or $y'' > 0$, which would indicate a nonrealistic geometry and a geometry with inflection points, respectively. An example of a polynomial generated body is shown in Figure 7 for a fineness ratio 5 body.

For a fineness ratio of 4, a range of prismatic coefficients and radii of curvature were tested. The investigation of fineness ratio 4 geometries was done to understand the influence that the prismatic coefficient and nose radius of curvature have on the power required to self-propel the bodies.

The very nature of this method enables it to be converted easily to a computer program. After conversion, a systematic procedure was developed to start with a geometry and result in a final C_p*. This method was also extended from a fifth-order to a sixth-order polynomial. As no significant improvement was shown, this was not pursued.

INVERSE METHOD

Included in the TAPS package is an inverse potential flow program developed by James[8] and the McDonnell-Douglas Corporation.[9,10] Input to the program is a velocity distribution, and by means of iteration a resulting geometry is output.

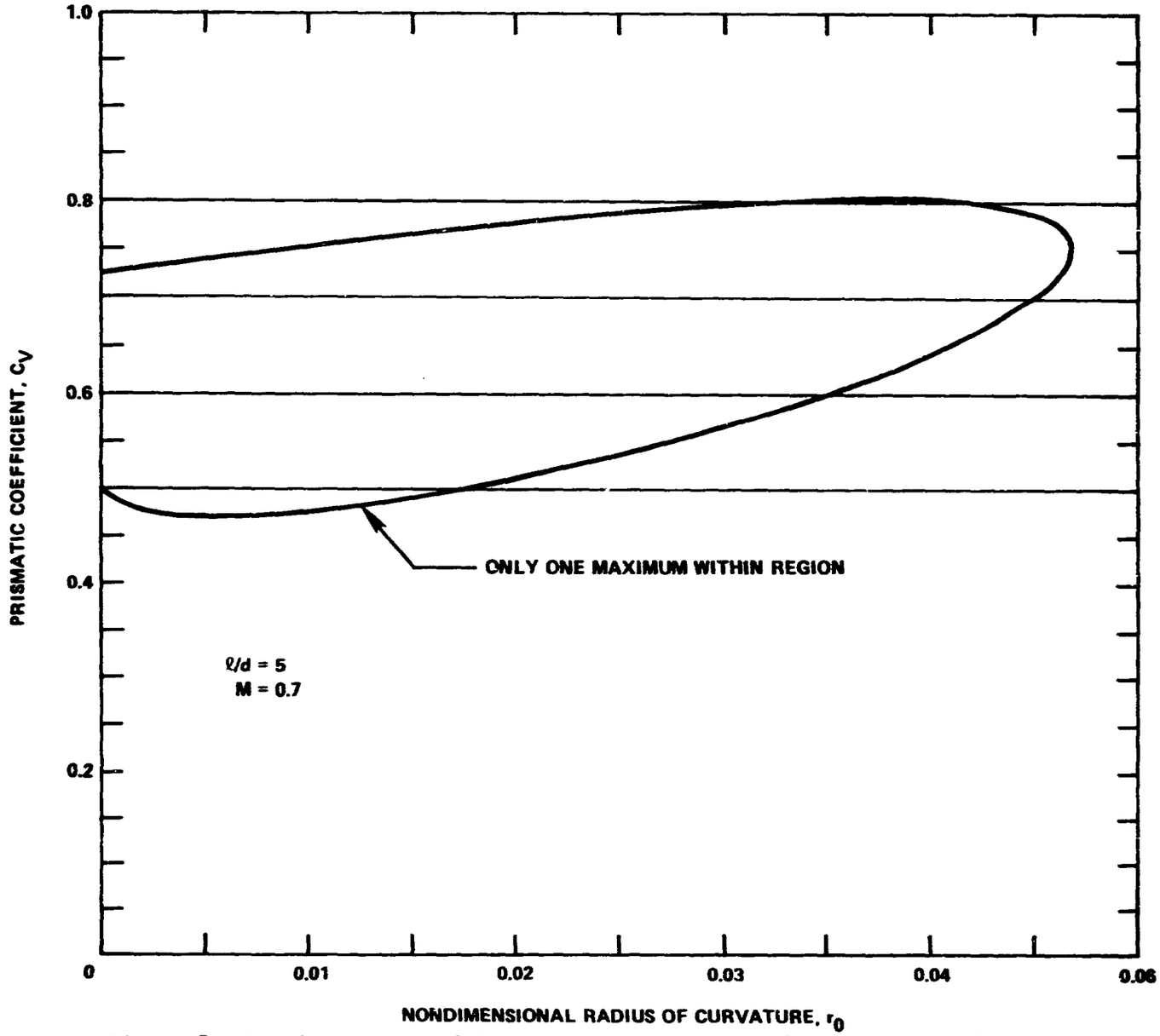

Figure 5 - Envelope Curve of Prismatic Coefficient and Nose Radius of Curvature Defined by Zero Slope Condition

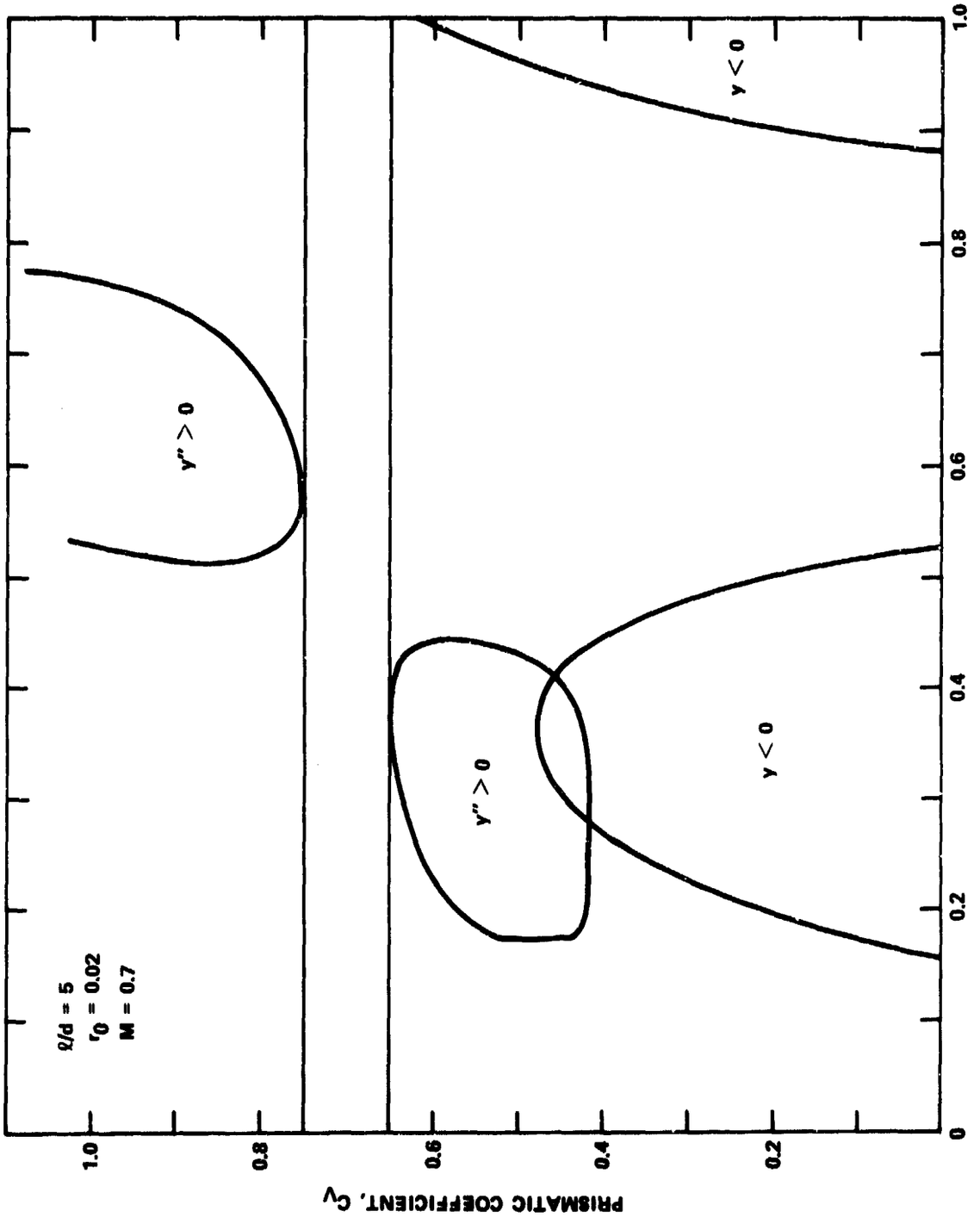

Figure 6 - Boundary Curves Defined by No-Inflection-Point and Positive y Condition

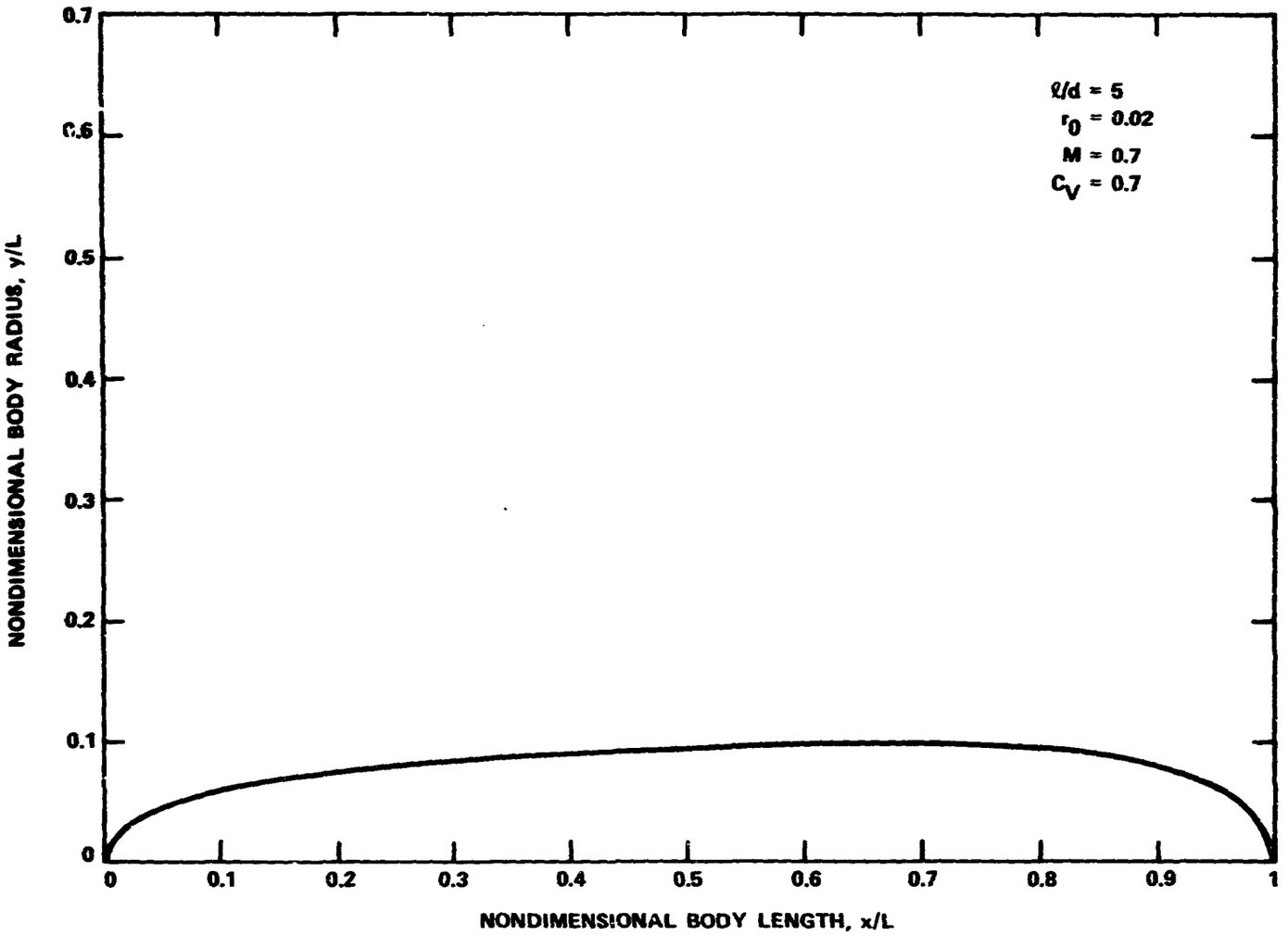

Figure 7 - Polynomial Generated Geometry

The following are sample input:

$$\left(\frac{V_l}{V}\right)^2 = K_1 \cdot S^{1/n} \qquad 0 \leq S < 1$$

$$\left(\frac{V_l}{V}\right)^2 = K_2 \qquad 1 < S \leq S_{te}$$

where S = 1 at the location of the inlet, and S = 0 at the nose.

By varying K_1, K_2, n, and S_{te} a family of velocity distributions can be generated (Figure 8).

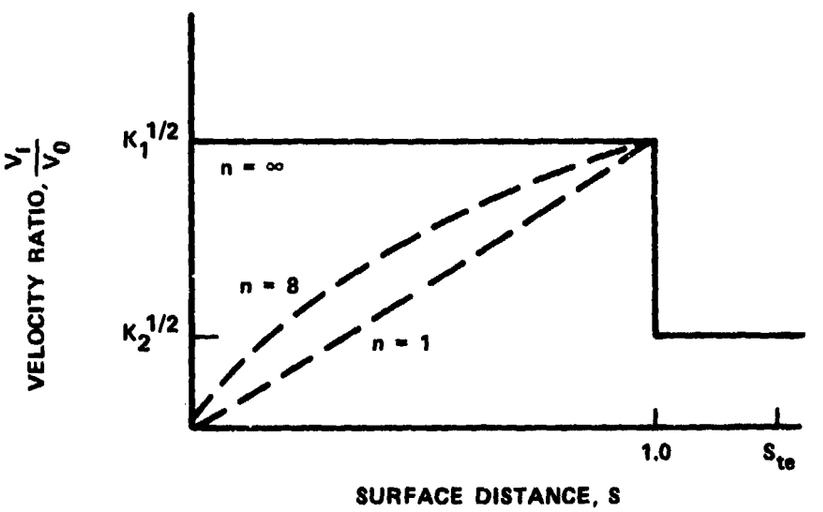

Figure 8 - Input Velocity Distribution

A numter of attempts were made using the TAPS inverse code, but the approach was discontinued due to unsatisfactory results. Subsequent analysis of an output geometry did not compare with the input velocity distribution. The failure of the TAPS inverse method is believed due to the convergence logic and its particular coding; therefore, a second inverse method was developed. This method, based on a surface discrete vortex distribution, was originally coded on a Tektronix terminal

for two-dimensional flow. Later, the method was developed for an axisymmetric flow and finally coded in FORTRAN for use on the CDC-6600-type computers.

The program receives as input a function for the body length. The function used was a series of straight lines; see Figure 9. The broken line in the figure results in a cusp-type of afterbody and is similar in shape to the velocity distribution for such a body. The solid line represents a symmetric velocity distribution (the type of input used in this analysis). The resulting geometry is symmetrical, which would change in shape based on changes in the slopes in the fore and aft input distribution. The resulting geometries were checked in the TAPS potential flow code to verify a flat velocity distribution. A sample result is shown in Figure 10.

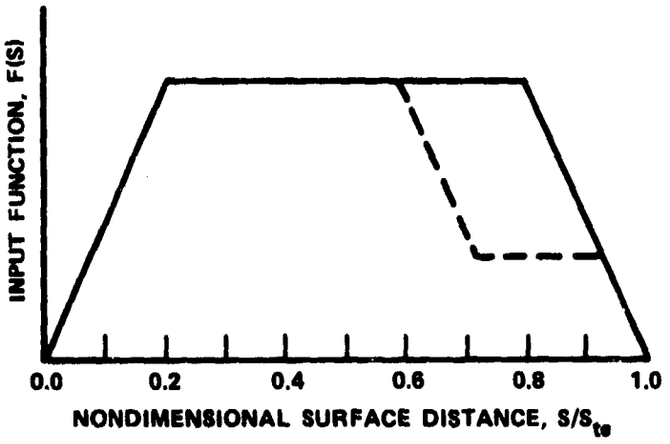

Figure 9 - Typical Input Function for Inverse Code

A number of other geometries were analyzed to put the final results in perspective. The laminar flow forebody shape of Goldschmied[11] was analyzed along with the wind tunnel model of fineness ratios of 4, 5, and 6.

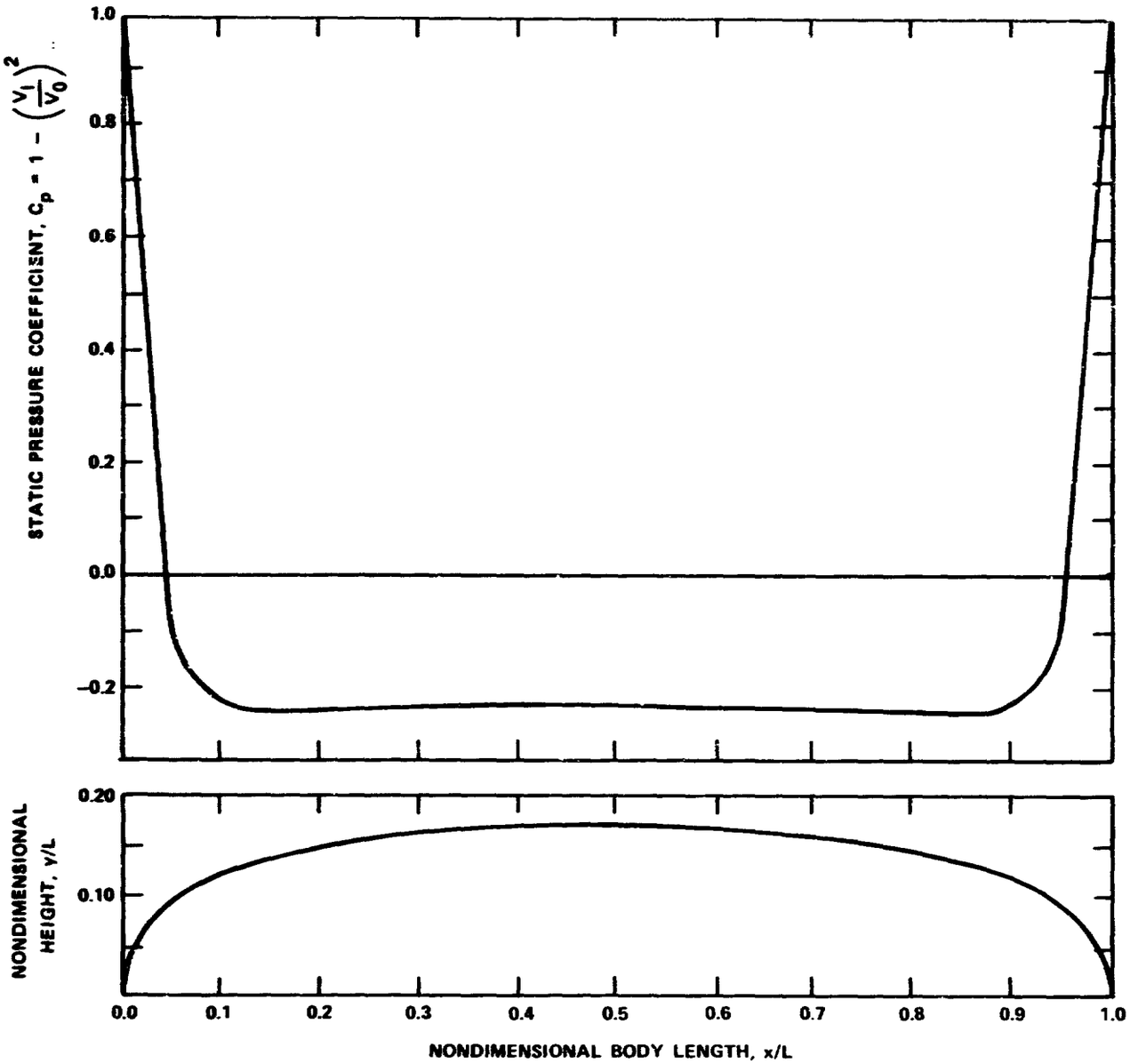

Figure 10 - Resulting Geometry and Corresponding Pressure Distribution from Inverse Code

RESULTS AND DISCUSSION

At low fineness ratios, the component of drag due to flow separation (residual drag) becomes more important. This phenomenon is seen in Figure 11 where the total drag of a typical Series 58 body is shown along with the components of drag, skin friction, and residual. Note that at the low fineness ratios the residual drag controls the shape of the total drag curve. By applying afterbody boundary layer control, the residual drag component can be eliminated, and the optimum fineness ratio for reducing propulsive power can be found based on a tradeoff of skin friction drag alone.

When attempting to reduce the skin friction of a body of revolution, there is a distinct tradeoff. By reducing fineness ratio, the wetted area required to enclose a given body is reduced as shown in Figure 12. This should reduce skin friction drag. However, reducing fineness ratio also increases the flow velocities over the surface, increasing skin friction drag. An analysis was conducted, using the methods previously described, to define the fineness ratio which optimizes the reduction in wetted area with the increase in surface velocity. (An assessment of a low drag spherical submersible was conducted at DTNSRDC in 1981.*)

The analysis was conducted as a two-step process. First, for a single fineness ratio, ($\ell/d = 4$), the influence of prismatic coefficient and nose radius of curvature was determined. The results in Table 2 show a range of less than 2 percent. Despite such a small range, it was apparent that the higher prismatic coefficient and nose radius of curvature bodies resulted in the lower power coefficients. This was the assumption used for the other fineness ratios.

---

*As documented by Leitner and McCabe in a report of higher classification.

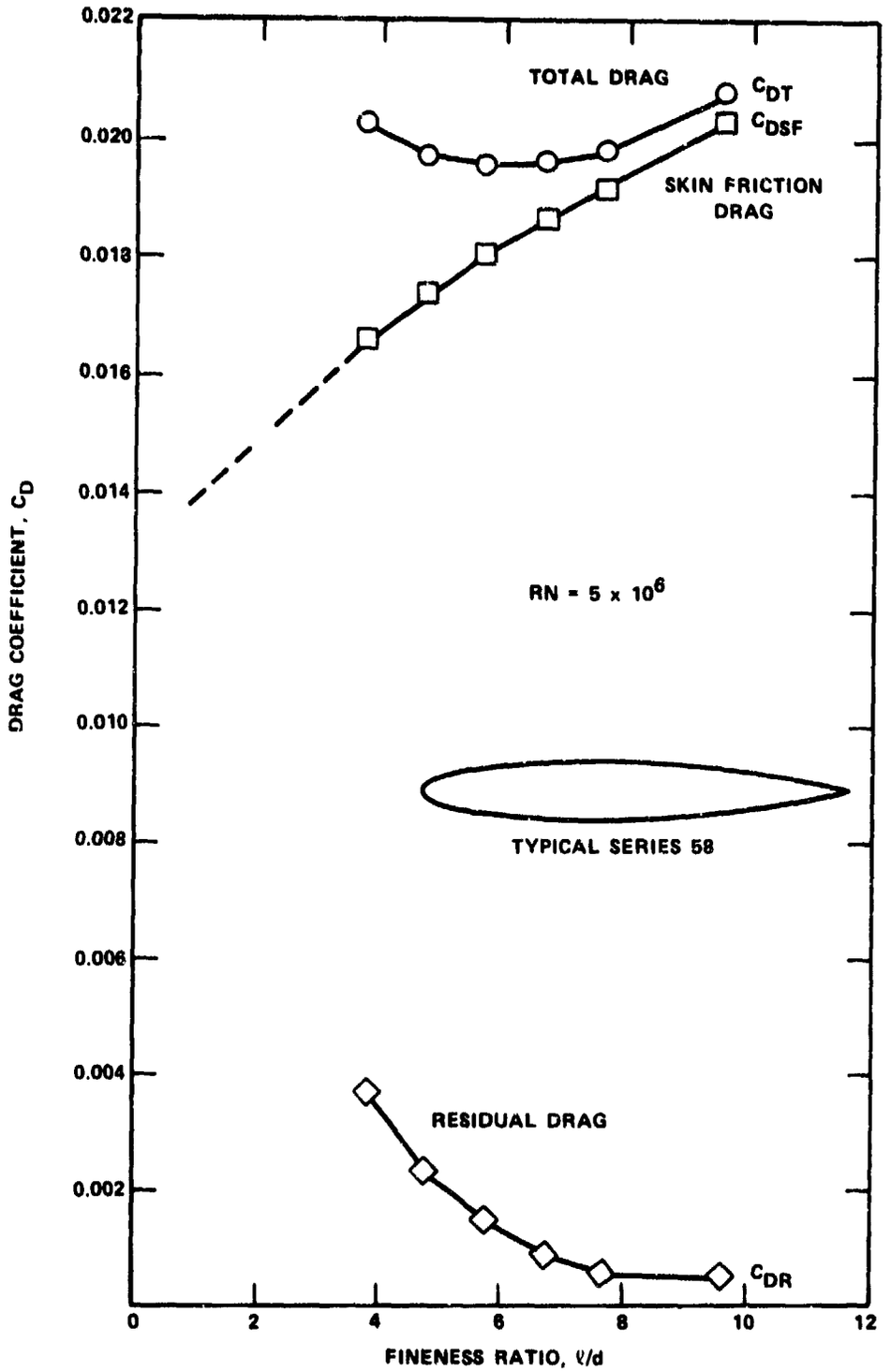

Figure 11 - Drag Coefficient versus Fineness Ratio for Series 58 Bodies

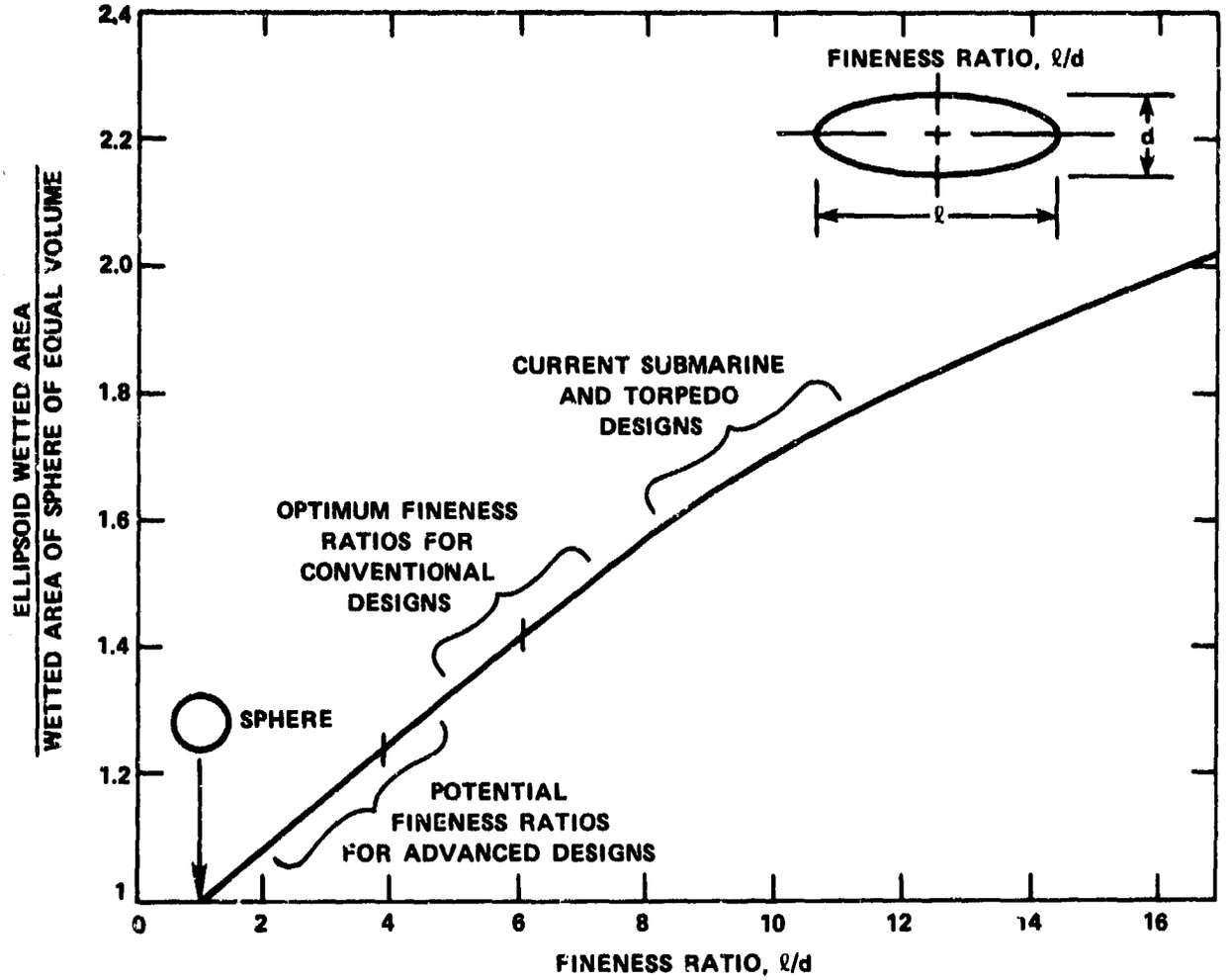

Figure 12 - Influence of Fineness Ratio on Wetted Area

TABLE 2 - PROPULSIVE POWER AS A FUNCTION OF PRISMATIC COEFFICIENT AND NOSE RADIUS OF CURVATURE
($\ell/d = 4$)

C_p*	C_V	r_o
0.01907	0.55	0.005
0.01897	0.60	0.005
0.01893		0.015
0.01894	0.65	0.005
0.01887		0.015
0.01883		0.025
0.01897	0.70	0.005
0.01893		0.015
0.01886		0.020
0.01879		0.035
0.01884	0.75	0.030
0.01882		0.035

The second step was to determine the influence of fineness ratio. The results of this analysis are shown in Figure 13 and Table 3. The primary method used was the polynomial generated shapes which make up the base-line curve. The polynomial shapes range from fineness ratios of 1 up to 10. Figure 13 also includes the various geometries used in the program analysis. The wind tunnel model with the Reichardt nose displays somewhat lower values than the base line. A third family of geometric shapes is shown with still lower propulsive power coefficient. These shapes, representing a flat pressure distribution, show an improvement of approximately 3 percent from the base line with a smaller improvement over the wind

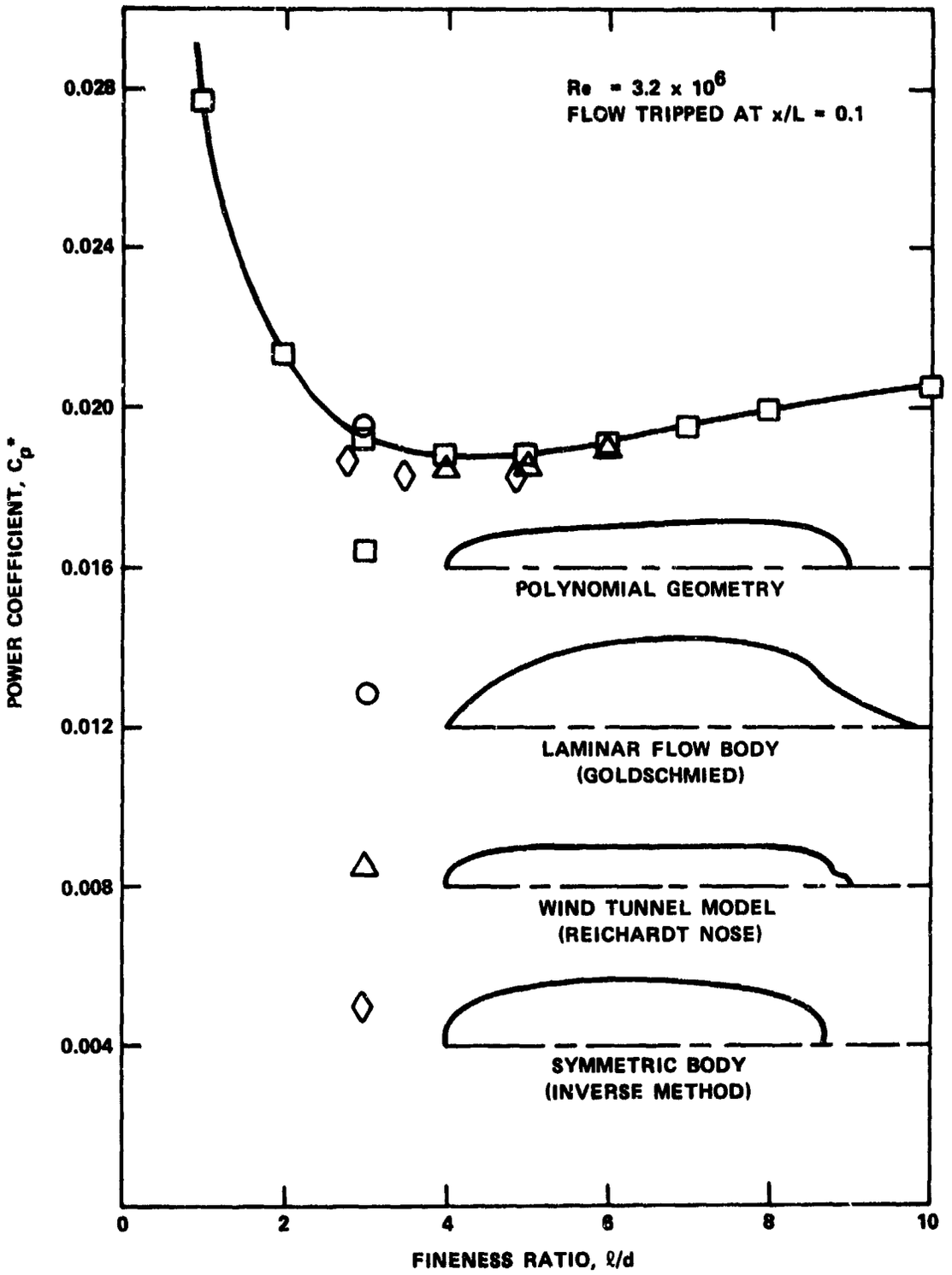

Figure 13 - Forebody Power Coefficient versus Fineness Ratio

tunnel model. The characteristic pressure distributions of these four geometries are shown in Figure 14.

TABLE 3 - TABULATED RESULTS OF POWER COEFFICIENT VERSUS FINENESS RATIO

ℓ/d	C_p^*	Geometry Type
1	0.02765	Polynomial geometry
2	0.02137	
3	0.01920	
4	0.01880	
5	0.01880	
6	0.01910	
7	0.01955	
8	0.01990	
10	0.02055	
4	0.01850	Wind tunnel model
5	0.01860	
6	0.01895	
2.8	0.01870	Symmetric body
3.5	0.01830	
4.9	0.01835	
3	0.01950	Goldschmied

CONCLUSIONS

Although the optimum fineness ratio appears to be 4, the curve is quite flat. An important consequence of this is that other design issues, which may necessitate changes in the vehicle's length or diameter, can be accommodated with impunity over a range of fineness ratios (2.5 to 8). (In practical terms, this relative

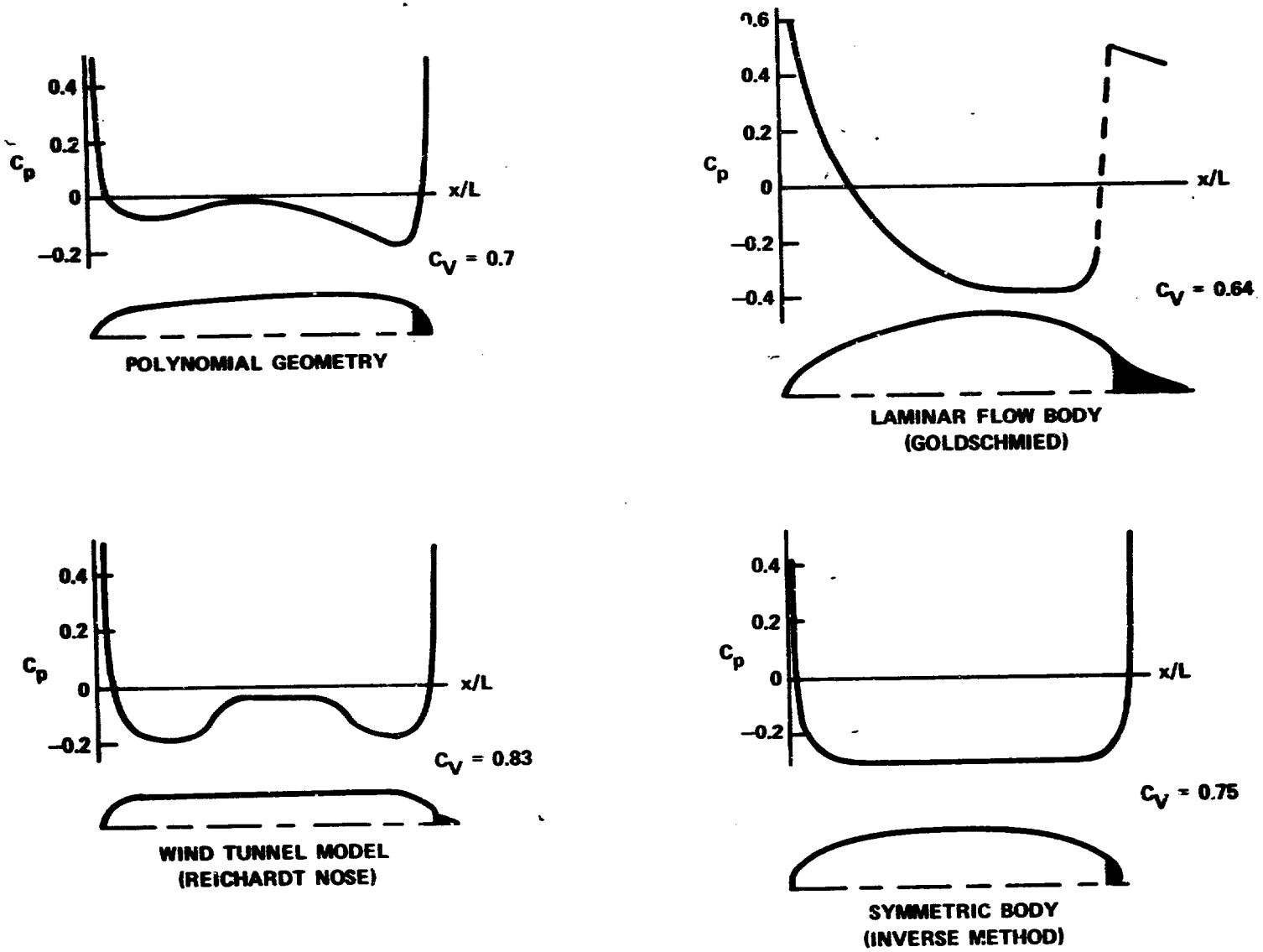

Figure 14 - Pressure Distribution of Various Geometries

insensitivity might extend to even lower fineness ratio bodies since the imposition of transition to turbulent flow at 10 percent body length may be overconservative for them. The sphere, for example, has a powerful favorable pressure gradient extending much further than 10 percent of length which might maintain a significantly greater region of laminar flow even in rather unfavorable practical conditions.)

For a constant fineness ratio, the different shapes varied by at most about 4 percent of C_p^*. Relative to the Reichardt shape selected for the wind tunnel model improvements of 1.5 percent were obtained.

By application of boundary layer control to underwater submersibles, a low-power vehicle can be designed with a fineness ratio of 2.5 and still have a high prismatic coefficient.

APPENDIX

FIFTH-ORDER POLYNOMIAL DERIVATION

The form of equation $y^2(x) = 2r_o R(x) + C_V P(x) + C^2 Q(x)$, which is the sectional area curve, is of the fifth order. The resultant meridian section can be easily defined by taking the square root of y^2. Substituting, f(x) for $y^2(x)$ gives the following boundary conditions:

a. $f(x = 0) = 0$

b. $f(x = 1) = 0$

c. $\frac{df}{dx}(x = 0) = 2r_o$

d. $f\ (x = M) = C^2$

e. $\frac{df}{dx}(x = M) = 0$

f. $\int_0^1 f(x)\,dx = C^2\ C_V$

where M = location of maximum thickness.

Since f(0) = 0, regardless of the values of r_o, C, and C_V,

$$R(0) = P(0) = Q(0) = 0 \tag{1}$$

Similarly, Equations (1) through (6) are obtained from:

Condition b

$$R(1) = P(1) = Q(1) = 0 \tag{2}$$

Condition c

$$R'(0) = 1,\ P'(0) = Q'(0) = 0 \tag{3}$$

where the prime denotes differentiation with respect to x.

Condition d

$$R(M) = P(M) = 0,\ Q(M) = 1 \tag{4}$$

Condition e

$$R'(M) = P'(M) = Q'(M) = 0 \tag{5}$$

Condition f

$$\int_0^1 R(x)dx = \int_0^1 Q(x)dx = 0, \quad \int_0^1 P(x)dx = C^2 \tag{6}$$

The values of R(x), P(x), and Q(x) are derived on the basis of the relation in Equations (1) through (6).

EVALUATION OF R(x)

Since $R(0) = R(M) = R'(M) = R(1) = 0$, and R(x) is a polynomial of the fifth degree, Equation (7) becomes

$$R(x) = x(x - 1)\ (x-M)^2(\alpha_o + \alpha_1 x) \tag{7}$$

The terms α_o and α_1 are solved from Equations (3) and (6). Substituting Equation (7) into Equation (3), $R'(0) = 1$,

$$\alpha_o = -\frac{1}{M^2} \tag{8}$$

Equation (7) can be written as

$$R(x) = \alpha_o\ [x^4 - x^3\ (2M + 1) + x^2\ (M^2 + 2M) - xM^2] \tag{9}$$

$$+ \alpha_1\ [x^5 - x^4\ (2M + 1) + x^3\ (M^2 + 2M) - x^2M^2]$$

Using this form of R(x) and applying Equation (6),

$$\int_0^1 R(x)\ dx = \alpha_o \left[\frac{1}{5} - \frac{1}{4}\ (2M + 1) + \frac{1}{3}\ (M^2 + 2M) - \frac{1}{2}\ M^2\right] \tag{10}$$

$$+ \alpha_1 \left[\frac{1}{6} - \frac{1}{5}\ (2M + 1) + \frac{1}{4}\ (M^2 + 2M) - \frac{1}{3}\ M^2\right] = 0$$

Then, applying Equation (8) and solving for α_1, .

$$\alpha_1 = \frac{-10M + 10M - 3}{M^2\ (-5M^2 + 6M - 2)} \tag{11}$$

EVALUATION OF P(x)

Since $P(0) = P'(0) = P(M) = P'(M) = P(1) = 0$, and since P(x) is a polynomial of the fifth degree, Equation (12) takes the form

$$P(x) = x^2 (x - M)^2 (x - 1) \beta_o \tag{12}$$

The term β_o is solved from Equation (6). By expanding Equation (12),

$$P(x) = \beta_o [x^5 - x^4 (2M + 1) + x^3 (M^2 + 2M) - x^2 M^2] \tag{13}$$

substituting into Equation (6),

$$\int_0^1 P(x)dx = C^2$$

$$= \beta_o \left[\frac{1}{6} - \frac{1}{5}(2M + 1) + \frac{1}{4}(M^2 + 2M) - \frac{1}{3}M^2\right] \tag{14}$$

Solving for β_o,

$$\beta_o = C^2 \Big/ \left[\frac{1}{6} - \frac{1}{5}(2M + 1) + \frac{1}{4}(M^2 + 2M) - \frac{1}{3}M^2\right] \tag{15}$$

EVALUATION OF Q(x)

Since $Q(0) = Q'(0) = Q(1) = 0$, and P(x) is a polynomial of the fifth degree, Equation (16) becomes

$$Q(x) = x^2(x-1) (\gamma_0 + \gamma_1 x + \gamma_2 x^2) \tag{16}$$

The terms γ_0, γ_1, and γ_2 are solved from Equations (4), (5), and (6). From Equation (4), $Q(M) = 1$, and

$$\gamma_o M^2 (M - 1) + \gamma_1 M^3 (M - 1) + \gamma_2 M^4 (M - 1) = 1 \tag{17}$$

Also, from Equation (5), $Q'(M) = 0$, and

$$\gamma_o M(3M - 2) + \gamma_1 M^2 (4M - 3) + \gamma_2 M^3 (5M - 4) = 0 \tag{18}$$

Equation (16) can be written as

$$Q(x) = \gamma_o (x^3 - x^2) + \gamma_1 (x^4 - x^3) + \gamma_2 (x^5 - x^4) \tag{19}$$

Finally, from Equation (6), $\int_0^1 Q(x)dx = 0$, and Equation (19),

$$\int_0^1 Q(x)dx = \gamma_o\left(\frac{1}{4} - \frac{1}{3}\right) + \gamma_1\left(\frac{1}{5} - \frac{1}{4}\right) + \gamma_2\left(\frac{1}{6} - \frac{1}{5}\right) = 0 \tag{20}$$

From Equations (17), (18), and (20), the system of three equations and three unknowns can be simplified and solved simultaneously for γ_o, γ_1, and γ_2. The resulting values are

$$\gamma_o = \frac{1 - 2.5M^2}{(1 - 1.5M)M} + \frac{12.5M^2 - 10M^2 - 3M + 2}{7.5M^3 - 6M^2 - 4M + 3} \tag{21}$$

$$\gamma_1 = \frac{1 - \gamma_o\,(1 - 2.5M^2)\,(M - 1)\,M^2}{M^3\,(M - 1)\,(1 - 1.5M)} \tag{22}$$

$$\gamma_2 = -\,(2.5\,\gamma_o + 1.5\,\gamma_1) \tag{23}$$

The set of equations to describe an axisymmetric body by means of a fifth-order polynomial can be summarized as

$$y^2 = 2r_oR(x) + C_VP(x) + C^2Q(x) \tag{24}$$

where

$$\begin{aligned} R(x) &= x(x - 1)\,(x - M)^2\,(\alpha_o + \alpha_1 x) \\ P(x) &= x^2(x - M)^2\,(x - 1)\,\beta_o \\ Q(x) &= x^2\,(x - 1)\,(\gamma_o + \gamma_1 x + \gamma_2 x^2) \end{aligned} \tag{25}$$

and

$$\alpha_o = -\frac{1}{M^2}$$

$$\alpha_1 = \frac{-10M^2 + 10M - 3}{M^2\,(-5M^2 + 6M - 2)}$$

$$\beta_o = C^2 \Big/ \left[\frac{1}{6} - \frac{1}{5}(2M + 1) + \frac{1}{4}(M^2 + 2M) - \frac{1}{3}M^2\right]$$

$$\gamma_o = \frac{1 - 2.5M^2}{(1-1.5M)M} + \frac{12.5M^3 - 10M^2 - 3M + 2}{7.5M^3 - 6M^2 - 4M + 3}$$

$$\gamma_1 = \frac{1 - \gamma_o\,(1 - 2.5M^2)\,(M - 1)M^2}{M^3(M - 1)\,(1 - 1.5M)}$$

$$\gamma_2 = -(2.5\gamma_o + 1.5\gamma_1)$$

As noted, not all combinations of r_o, C_V, C, and M define shapes that are either realistic or smooth. To ensure a satisfactory shape, equations have been defined that must be satisfied. These restrictions, which are the same as those imposed in Reference 7, include the existence of a single maxima between the nose and tail of the body and at a prescribed location, M. Also, y must always be greater than zero, and the slope of the body must continuously be decreasing as x goes from nose to tail.

REFERENCES

1. Neumann, B.J., "Application and Correlation of Currently Available Design Tools for an Axisymmetric Underwater Vehicle with Boundary Layer Control," DTNSRDC/ASED-83/05 (In preparation).

2. McCabe, E.F., Jr. and B.J. Neumann, "Performance Evaluation Data for a Parametric Integrated BLC/Propulsive Afterbody AUV Model," DTNSRDC/ASED-83/03 (In preparation).

3. Hess, J.L. et al., "On The Problem of Shaping an Axisymmetric Body to Obtain Low Drag at Large Reynolds Numbers," McDonnell-Douglas Corporation Report MDC J6791 (Jan 1975).

4. Parson, J.S. and R.E. Goodson, "The Optimum Shaping of Axisymmetric Bodies for Minimum Drag in Incompressible Flow," Purdue University Report ACC-72-5 (Jun 1972).

5. Gentry, A.E., "The Transition Analysis Program System: Volume 1 - User's Manual," McDonnell-Douglas Corporation Report MDC J7255/01 (Jun 1976).

6. Gentry, A.E. and A.R. Wazzan, "The Transition Analysis Program System: Volume 2 - Program Formulation and Listings," McDonnell-Douglas Corporation Report MDCJ72555/02 (Jun 1976).

7. Gertler, M. and Landweber, L. "Mathematical Formulation of Bodies of Revolution," DTMB Report 719 (Sep 1950).

8. James, R.M., "A General Analytical Method for Axisymmetric Incompressible Potential Flow about Bodies of Revolution," Computer Methods in Applied Mechanics and Engineering, Vol. 12, No. 1 (Sep 1977).

9. Cebeci, T. et al., "Boundary Layer and Inverse Potential Flow Methods for Axisymmetric Bodies," McDonnell-Douglas Corporation Report MDC J7895 (Mar 1978).

10. Lee, R.S. and W.A. Anderson, "The Transition Analysis Program System - Addendum 1," McDonnell-Douglas Corporation Report MDC G7548 (Jun 1978).

11. Goldschmied, "Integrated Hull Design, Boundary-Layer Control and Propulsion of Submerged Bodies," AIAA Journal of Hydronautics, Vol. 1, No. 1 (Jul 1967).

INITIAL DISTRIBUTION

Copies	
6	DARPA 3 Program Management/Mgt Info Systems 3 Strategic Tech Office/ R. Leitner
1	NRL
1	NAVSEASYSCOM SEA-63R31/T. Peirce
1	NUSC 3634/R. Nadolink
12	DTIC
1	Penn State University Applied Res Lab/R. Henderson
1	TACTEC
1	The Charles Stark Draper Laboratory, Inc./M. O'Brien
1	RAMCOR, Inc./P. Georgallis

CENTER DISTRIBUTION

Copies	Code	Name
1	012.3	D. Jewell
1	012.4	H. Jacobs
1	014	
1	154	
1	1544	R. Boswell
1	1556	
16	1603	B. Neumann
1	1606	C. Applegate
2	1606	Aerodynamics Collection
1	1843	H. Haussling
1	1920	R. Biancardi
10	5211.1	Reports Distribution
1	522.1	Unclassified Library (C) + 1M
1	522.2	Unclassified Library (A)
1	93	Patent Counsel

[illegible] ISSUES THREE TYPES OF REPORTS

1. [illegible] REPORTS, A FORMAL SERIES, CONTAIN INFORMATION OF PERMANENT TECHNICAL VALUE. THEY CARRY A CONSECUTIVE NUMERICAL IDENTIFICATION REGARDLESS OF THEIR CLASSIFICATION OR THE ORIGINATING DEPARTMENT.

2. DEPARTMENTAL REPORTS, A SEMIFORMAL SERIES, CONTAIN INFORMATION OF A PRELIMINARY, TEMPORARY, OR PROPRIETARY NATURE OR OF LIMITED INTEREST OR SIGNIFICANCE. THEY CARRY A DEPARTMENTAL ALPHANUMERICAL IDENTIFICATION.

3. TECHNICAL MEMORANDA, AN INFORMAL SERIES, CONTAIN TECHNICAL DOCUMENTATION OF LIMITED USE AND INTEREST. THEY ARE PRIMARILY WORKING PAPERS INTENDED FOR INTERNAL USE. THEY CARRY AN IDENTIFYING NUMBER WHICH INDICATES THEIR TYPE AND THE NUMERICAL CODE OF THE ORIGINATING DEPARTMENT. ANY DISTRIBUTION OUTSIDE [illegible] MUST BE APPROVED BY THE HEAD OF THE ORIGINATING DEPARTMENT ON A CASE-BY-CASE BASIS.